Control of Nonlinear Dynamics of Quantum Dot Laser with External Optical Feedback

H. Al Husseini*

Nassiriya Nanotechnology Research Laboratory (NNRL), Science College, Thi-Qar University, Nassiriya, Iraq

Abstract: We examine the nonlinear dynamics of a semiconductor quantum-dot (QD) laser subject to external optical feedback by using dimensionless equations numerical model. In our QD laser model we employ dynamic for ground and excited state processes, additionally between the QDs and the wetting layer (WL). This enables us to tune the output of external cavity modes QDs by changing the bias current, delayed time and feedback strength to investigate how they affect the stability properties of the QD laser. Our results show that high bias current and small α-factor value lead to lower sensitivity of the laser towards optical feedback.

Keywords: Quantum-dot (QD) laser, dynamics, optical feedback.

1. INTRODUCTION

One particularity of semiconductor lasers is their low tolerance to optical feedback, which can be of disadvantage for technological applications. For example, to use semiconductor lasers as transmitters in optical networks, expensive optical isolators are needed to avoid back reflections that can lead to temporal instabilities of the lasers (coherence collapse).

However, there are also several applications that take advantage of the rich dynamics induced by optical feedback. For instance, feedback induced chaos can be used for secure chaos communication and chaos key distribution [1-6]. Furthermore, short optical feedback in an integrated multi-section laser has been used to significantly improve the modulation bandwidth of a directly modulated laser [7].

Moreover, from a dynamical system point of view, semiconductor lasers subject to optical feedback are of high interest, because the optical feedback introduces a delay into the system. The delay in turn induces a high dimensionality, which results in a rich phenomenology, ranging from multistability, bursting, intermittency, irregular intensity dropouts (low-frequency fluctuations LFFs), and fully developed chaos.

A review focusing on laser instabilities is given in [8]. Semiconductor lasers have also been employed to demonstrate the stabilization of steady states (cw emission) or periodic oscillations (self-pulsations) by non-invasive time delayed feedback control [9-14] (see [15, 16] for an overview). Further, delay synchronization of coupled lasers [17], and networks of delay coupled lasers [18, 19] as well as bubbling in coupled lasers [20, 21] have been investigated. A recent review summarizing the dynamics and the applications of delay coupled lasers is given in [22]. QD lasers display a higher dynamical stability with respect to optical feedback [23-27] than conventional QW semiconductor lasers. This allows QD laser transmitters to operate without expensive optical isolators [28]. Furthermore, due to their increased dynamical stability, the route to chaos can be observed in QD lasers more clearly. The improved performance of QDs under optical feedback has been linked to an increased RO damping and a reduced phase-amplitude coupling [29-32].

So in our rate equation model, we exceed the rate equations to a ground and exited states (ρ_{gs}, ρ_{es}), and a single non-resonant population N_{wl}. Due to Pauli blocking, the number of available states in the dot are limited on two states. In addition, the occupancy of the dot plays a major part on capture rate of charge carrier. Therefore, the model is based on the assumption that the carriers are directly injected into the wetting layer (WL) of the device, so that they can be captured into the QDs. Furthermore, the model neglects the charge carrier transport without the active region. A similar approximation was used in the QW devices [33].

The paper is organized as follows: Before we perform any numerical bifurcation studies we introduce the QD laser model with external optical feedback in Sec. II. In Section III, we summarize the results for Ɛ = 0. The next two sections are devoted to the study of the full delay differential equation (DDE) for Ɛ ≥ 0. Section IV presents numerical results on basic bifurcations of bias current and delay time. Sections V is devoted to bifurcation diagrams for two representative values of

*Address correspondence to this author at the Nassiriya Nanotechnology Research Laboratory (NNRL), Science College, Thi-Qar University, Nassiriya, Iraq; E-mail: alhusseini_2007@yahoo.com

E-ISSN: 2311-8792/16

the linewidth enhancement factor α, and Θ. Finally, we summarize in Section VI.

2. QUANTUM DOT LASER MODEL

The rate equations for a QD laser subject to optical feedback formulated by O'Brien *et al*. [29] consist of three equations for the amplitude of the normalized laser field in the cavity E, the occupation probability ρ of a QD in the laser, and the number n of carriers in the reservoir per QD. The carriers are first injected into the quantum well before being captured into the QD as previously used in other models describing QD laser dynamics [34, 35]. However, because of Pauli blocking, the capture rate depends on the occupancy level of the QDs. The system with a ground and exited states in the QDs can be described with the following rate equations:

$$E^{\bullet} = -\frac{1}{2}\gamma_s E - \frac{1}{2}(1+i\alpha)\upsilon g_o(2\rho_{gs}-1)E + \frac{1}{2}\gamma E_\tau e^{-i\Theta}. \quad (1.a)$$

$$\rho_{gs}^{\bullet} = \gamma_{c_{es}}\rho_{es}(1-\rho_{gs}) - \gamma_d\rho_{gs} - g_o(2\rho_{gs}-1)|E|^2 \quad (1.b)$$

$$\rho_{es}^{\bullet} = \gamma_{c_{wl}} N_{wl}(1-\rho_{es}) - \gamma_d\rho_{es} - \gamma_{c_{es}}\rho_{es}(1-\rho_{gs}) \quad (1.c)$$

$$N_{wl}^{\bullet} = \frac{J}{e} - \gamma_n N_{wl} - 2\gamma_{c_{wl}} N_{wl}(1-\rho_{es}) \quad (1.d)$$

where the dot denotes derivation with respect to time. The band diagram of the model used here is shown in

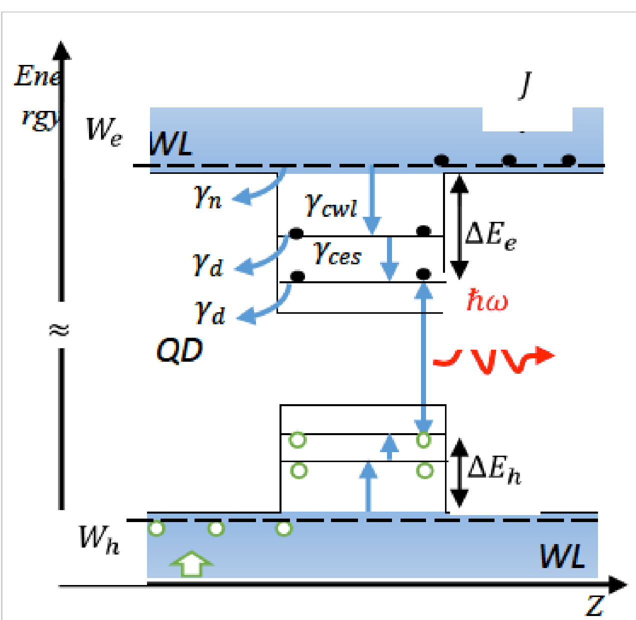

Figure 1: Schematic energy band diagram of QW and QD. ΔE_e, ΔE_h denote the energy spacing of the QW band edge and the QD ground state (GS) for electrons and holes. $\hbar\omega$ marks the GS lasing energy of the QD.

Figure **1**. Here, $E(t) = \sqrt{S}e^{-i\Phi(t)}$ is the normalized slowly varying complex amplitude of the electrical field given in polar coordinates by the photon number S and the phase Φ, and time t is scaled with ω_r^{-1}, where ω_r is the frequency of the relaxation oscillation, an intrinsic resonance of the optical mode. γ_s is the photon decay rate in the cavity. The parameter α is the linewidth enhancement factor, $g_o = \sigma v_g$, where σ is the cross section of interaction of carriers in the dots with photons; v_g is the group velocity; and $\upsilon = 2N_d\Gamma/d$, where Γ is the confinement factor and d is the thickness of the dot layer.

N_d is the two-dimensional density of dots. Although being completely determined by w_o and τ the feedback phase Θ is treated as an independent parameter since small variations of the external cavity length cause a variation of the phase Θ over its full range [0; 2π] while the external roundtrip time τ is hardly affected by these fluctuations. This is a well-established procedure in the analysis of semiconductor lasers subject to optical feedback [36-39]. Hence, we always consider Θ as a free parameter in our two-parameter bifurcation diagrams presented in Sec. IV and V. The parameter γ measures the injected field strength. The phase shift of the light during one round trip in the external cavity ($\tau = 2L/c$) is given by $\Theta = \omega_o\tau$, c is the speed of light. With w_o denoting the frequency of the solitary laser at the lasing threshold. The field labeled by the subscript τ, E_τ, and there with ϕ_τ, are the electric field amplitude and the optical phase taken at the delayed time t-τ. ρ_{gs} and ρ_{es} are the occupation probability in a ground and exited states in the quantum dots; N_{wl} is the carrier density in the well; γ_n and γ_d are the non-radiative decay rates for carriers in the WL and dot respectively; γ_{cwl} and γ_{ces} are the capture rate from wetting layer into an empty exited state and from exited into ground states respectively. J is the electrically injected pump current per dot, and it is the control parameter, q is elementary charge. The last terms in Eqs. (1.c) and (1.d) describe the rate of exchange of carriers between a ground and exited states in the dots and between the well and the exited state in the dots. Here we show that the mechanism for the capture of carriers into the dots can significantly alter the damping rate of the relaxation oscillations and, as a result, reduce the sensitivity to optical feedback. Carrier escape from the dots can be ignored because it is a temperature-dependent function controlling. This leads to a carrier capture time from the well that is dependent on the occupation probability of the dots.

The field equation is a complex stochastic differential equation. The goal is to transform the complex stochastic differential equation for E (Eq. 1.a) into two real stochastic differential equations for the photon density $S = |E|^2$ and the phase *Φ*. Neglecting the stochastic term this is just a transformation to polar coordinates. Averaging over the stochastic terms the final rate equations for the photon density *S*, the phase of the electric field *Φ*, and the three equations for the occupation probability of a ground and exited states in the QDs (ρ_{gs} and ρ_{es}) and carrier density in the WL (N_{wl}) read:

$$S^{\bullet} = [\upsilon g_o(2\rho_{gs}-1)-\gamma_s]S + \gamma\sqrt{SS_\tau}\cos(\phi-\phi_\tau) \qquad (2.a)$$

$$\phi^{\bullet} = -\frac{\alpha}{2}\upsilon g_o(2\rho_{gs}-1) - \frac{\gamma}{2}\sqrt{S_\tau / S}\sin(\phi-\phi_\tau) \qquad (2.b)$$

$$\rho_{gs}^{\bullet} = \gamma_{c_{es}}\rho_{es}(1-\rho_{gs}) - \gamma_d\rho_{gs} - g_o(2\rho_{gs}-1)S \qquad (2.c)$$

$$\rho_{es}^{\bullet} = \gamma_{c_{wl}}N_{wl}(1-\rho_{es}) - \gamma_d\rho_{es} - \gamma_{c_{es}}\rho_{es}(1-\rho_{gs}) \qquad (2.d)$$

$$N_{wl}^{\bullet} = \frac{J}{e} - \gamma_n N_{wl} - 2\gamma_{c_{wl}}N_{wl}(1-\rho_{es}) \qquad (2.e)$$

In our approach, the carrier-light interaction is summarized in the photon density *S*, which includes all longitudinal modes. The factor 2 in Eq. (2.e) accounts for the twofold spin degeneracy in the quantum dot energy levels. A similar factor 2 is included in the definition of the differential gain factor *g* in Eq. (2.a) [40]. For numerical purposes, it is useful to rewrite Eqs. (2) In dimensionless form. To this end, we introduce the new variables;

$$x = \frac{g_o}{\gamma_d}S,\ \Phi \equiv \Phi,\ y = \frac{g_o\upsilon}{\gamma_s}(2\rho_{gs}-1),$$

$$z \equiv \rho_{es},\ w = \frac{\gamma_{c_{wl}}}{g_o\upsilon}N_{wl},$$

$$\Gamma = \frac{\gamma_{c_{es}}}{\gamma_s},\ \Gamma_1 = \frac{g_o\upsilon}{\gamma_s}, \Gamma_2 = \frac{\gamma_d}{\gamma_s},$$

$$\Gamma_3 = \frac{\gamma_{c_{wl}}}{\gamma_s},\ \Gamma_4 = \frac{\gamma_n}{\gamma_s},$$

$\delta_o = \dfrac{J}{g_o\upsilon q}$ and the time scale $t' = \gamma_s t$. The rate;

$$x^{\bullet} = x(y-1) + \varepsilon\sqrt{x x_\tau}\cos(\phi-\phi_\tau) \qquad (3.a)$$

$$\Phi^{\bullet} = -\frac{\alpha}{2}y - \frac{\varepsilon}{2}\sqrt{x_\tau / x}\sin(\phi-\phi_\tau) \qquad (3.b)$$

$$y^{\bullet} = \Gamma z(\Gamma_1 - y) - \Gamma_2 y(1+2x) - \Gamma_1\Gamma_2 \qquad (3.c)$$

$$z^{\bullet} = \Gamma_1 w(1-z) - \Gamma_2 z - \Gamma z(1-y/\Gamma_1)/2 \qquad (3.d)$$

$$w^{\bullet} = \Gamma_3\delta_o - \Gamma_4 w - 2\Gamma_3 w(1-z) \qquad (3.e)$$

Where $\varepsilon = \gamma/\gamma_s$. The well-established assumptions here are that the delay time τ is larger than the laser roundtrip time inside the active region (Figure **1**). Then, five coupled equations are essential for QD laser with external optical feedback and they show unstable oscillations and chaotic dynamics in their output powers like three coupled equations in Lorenz systems. This is shown by the corresponding the inter-spike interval (ISI) probability distribution which consisting of an exponentially decaying function of the time, typical of random processes, displaced by the pulse duration, acting as a refractory time. In the numerical simulations, the fourth-order Runge-Kutta algorithm is used, Graphics Berkeley Madonna and Origin version 8.5 software are used to analyze the time series generated in the chaos regime. The analysis concerns the study of the attractors and the bifurcation scenario of the output laser. The parameter values used in the simulations are given in Table **1**.

Table 1: Numerical Parameters Used in the Simulation Unless Stated Otherwise

Parameters	Value	Parameters	Value
x_o	0.04	Γ_2	0.07
Φ_o	0.04	Γ_3	5.32
y_o	0.8	Γ_4	0.037
z_o	0.51	α	0.9
w_o	0.049	τ	5.78
Γ	8.12	ε	0. 35
Γ_1	1.79	δ_o	0.17

3. NUMERICAL RESULTS

The corresponding turn-on dynamics of the QD-laser without optical feedback ($\mathcal{E}$ = 0, in this case the evolution of the intensity and carrier densities do not depend on the phase of the electric field) obtained by numerical integration of Eqs. (3a-e) is shown in Figure **2**. The assumed values of all numerical parameters appearing in Eqs. (3a-e) are listed in Table **1**. If not stated otherwise they will be used for all subsequent simulations and path continuations. The

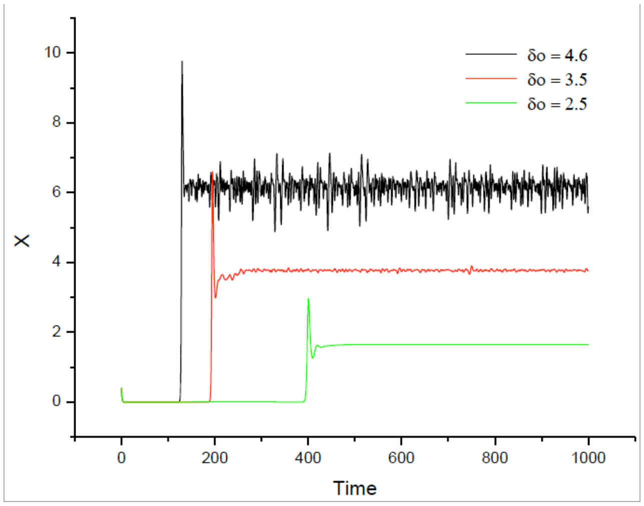

Figure 2: Turn-on dynamics of the QD laser without optical feedback. The bias current varies from δ_O = 2.5 (Green) the steady state to δ_O = 4.6 (Black) spiking. And the QD-QW parameters are changed in agreement with Table **1**.

important difference between the three turn-on curves in Figure **2,** is the damping of the relaxation oscillations. The colored line that corresponds to exponential decay of the photon density to its steady state value dependence of bias current values. This is the characteristically turn-on behavior of a QD laser corresponding to difference values of parameters (δ_O). Hence, this QD structure is labeled fast because increase bias current imply fast carrier exchange between QD and QW, here the difference rely only one variable to generate spikes. The turn-on dynamic of the reference QD structure shows relaxation oscillations that are more strongly damped than in the case of slow carriers but still observable. This case is called reference as it resembles the behavior found in common QD laser experiments [41]. It was investigated in previous dynamical studies of the QD laser with optical feedback [42, 43].

4. TURN-ON DYNAMICS OF TWO-PARAMETER BIFURCATIONS

Our QD laser model in the form of Eqs. (3a-e) for Ɛ = 0 is described in Sec. III. In this section, we discuss

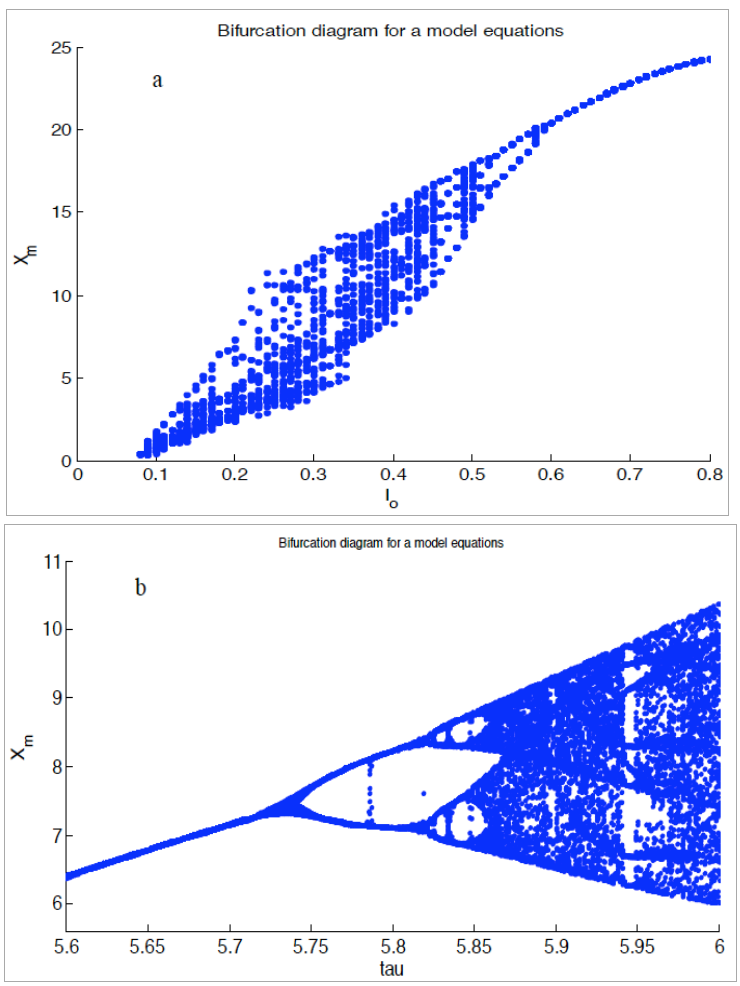

Figure 3: two-parameter bifurcation diagrams of the photon number x vs. bias current for direct numerical DDE (a), the QD-QW parameters are changed in agreement with Table **1**. And vs. delayed time (b), further parameter are fixed at w_O = 0, Ɛ = 0.312, δo = 0.281.

the turn-on dynamics of QD lasers of the DDEs for $\mathcal{E} \geq 0$ in two different parameters values: (i) in a configuration where there is bias current variable but with the same carrier lifetime and (ii) in a configuration where delayed time outside regions act as the affect factor (as in Figure **3**). It is this element of infinite dimensionality that allows Eqs. (3a-e) to show much richer dynamics than the QD laser alone (when $\mathcal{E} = 0$).

In light of the explicit split into slow and fast variables of the system, what is presented here is a case study of a slow–fast system subject to delayed feedback. This more general aspect provides a second motivation, because it may also be of interest for other areas of application. For example, the issue of delayed feedback or coupling also arises in the context of interacting (populations of) neuron cells, which themselves may display dynamics on separate timescales.

If we begin our analysis with the upper bifurcation diagram of Figure **3**(**a**), from the figure, when the injection current is increased, one recognizes that the value of the steady-state solution of the carrier density is increased and the laser tends to be less sensitive to the feedback light. Finally, the laser reached stable oscillation state even in the presence of feedback. In optical feedback, the laser tends to less unstable for the increase of the bias injection current, but instabilities of the laser persist and never disappear. This is the big difference between bulk and QD laser with optical feedback. This is in contrast to the dynamics of coherent output with feedback, where a significant shift and broadening of these peaks occurs for increasing bias injection current. The clear difference behavior of bifurcation diagram shown in Figure **3**(**b**). For increasing delayed time τ of lower bifurcation diagram becomes unstable in a Hopf bifurcation and the emerging periodic orbit bifurcates *via* period doubling.

4. TURN-ON DYNAMICS OF TWO-PARAMETER BIFURCATIONS

This section will discuss the dynamics of the QD laser as a function of feedback strength $\mathcal{E}$ and the linewidth enhancement factor α. As mentioned above modeling the short cavity regime results in sensitivity of the laser output to the phase Θ of the electric field. The feedback phase is fixed to π. and is only treated as a tunable parameter in Section II. Numerically obtained bifurcation diagrams as well as time series, ISI, and attractors will be discussed in order to elucidate the internal dynamics of the laser.

4.1. For $\Theta = 0$ and $\alpha = 0.9$

In the following simulations the dynamics of the QD laser with feedback is pumped at a bias current of $\delta o = 0.17$. For gradually increasing feedback strength $\mathcal{E}$ the local minima and maxima of the laser output, i.e., of the photon density, are recorded starting at time $t = 0$ and plotted in a bifurcation diagram as shown in Figure **4**. Note that the long integration time is chosen in order to avoid transient effects of the turn-on dynamics in the laser output.

For small $\mathcal{E} < 0.24$ the laser shows steady state operation at the first external cavity modes. At $\mathcal{E} = 0.24$ the external cavity modes loses stability in a supercritical Hopf bifurcation leading to a small stable limit cycle, i.e., to a solution with periodically modulated photon density. Thus, the bifurcation diagram for

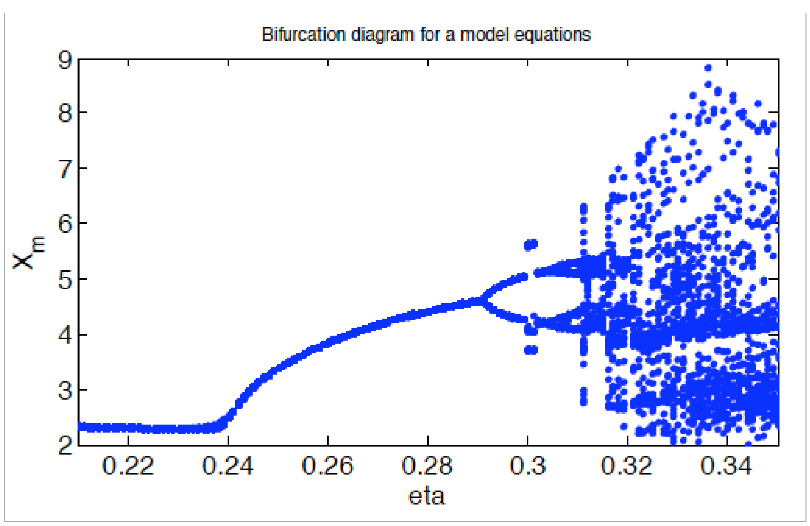

Figure 4: Bifurcation diagrams of the photon density x dependence of the feedback strength $\mathcal{E}$ for small $\alpha = 0.9$.

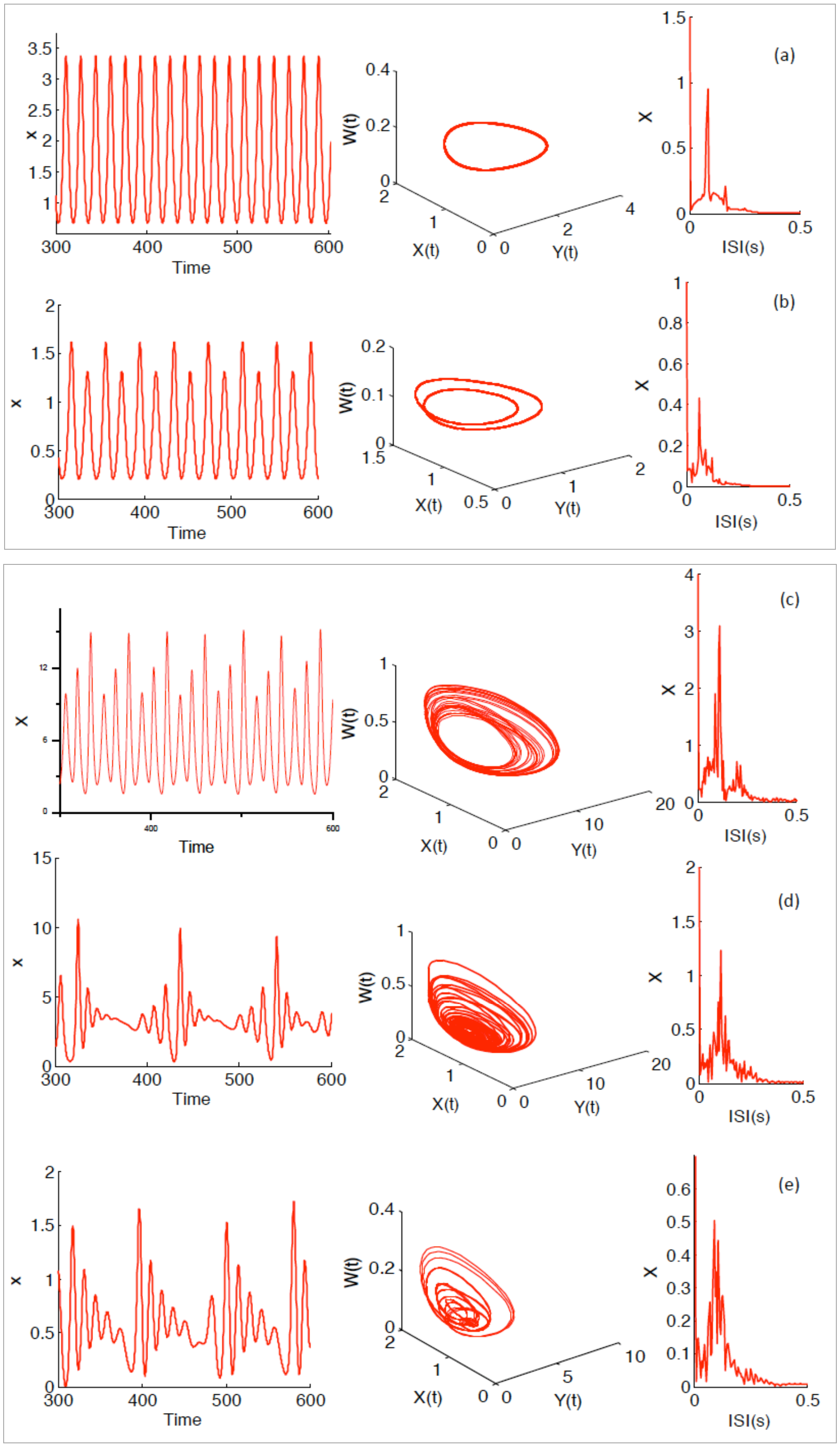

Figure 5: Time series (left), attractors and ISI (right) for selected feedback strengths $\mathcal{E}$: rows (a–e) correspond to $\mathcal{E}$ = 0.25-0.31 as indicated by the bifurcation diagram for small α = 0.9 and δo = 0.17 in Figure **4**.

$\mathcal{E}$ > 0.29 (see Figure **4** and the blowup Figure **5**) shows two branches: the maxima and minima of the limit cycle oscillations. The two branches scale like the square root of the distance from the bifurcation point. This is the signature of a Hopf bifurcation. For $\mathcal{E}$ = 0.22 time series, attractor and ISI of these periodic pulsations are shown in Figure **5a** (corresponding to the Figure **4**). With further increase of the feedback strength $\mathcal{E}$ the system undergoes a period doubling route to chaos with windows of period two and three at Ɛ = 0.3 and

0.31 that are indicated as in the bifurcation diagram (Figure **3**). The corresponding time series, attractors and ISI are depicted in Figure **5b** and **c**, respectively. They correspond to two folded and three folded limit cycles in the phase space projection shown in Figure **5b** and **c**. At Ɛ = 0.31 (d) the laser output is chaotic (dense dots at fixed Ɛ in the bifurcation diagram Figure **4**), which can also be seen in the broad spectrum of Figure **5** and the large chaotic attractor in the phase space projections (Figure **5**). The time series displays irregular pulse packages that are modulated with the frequency of the relaxation oscillations. This results in an erratic—sensitive to initial conditions—sequence of homoclinic-like spikes on top of a chaotic background (Figure **5d**). The corresponding ISI histogram (Figure **5d**) shows that the aperiodic (chaotic) background triggers the spikes in an erratic sequence, as indicated by its exponential tails. However, on top of this background the ISI histogram displays a complicated structure of sharp peaks revealing the complex structure of unstable periodic orbits embedded in the chaotic attractor nonlinearly by the Ɛ.

Figure **5a** is show only one single period beyond $\mathcal{E}$ = 0.24. In a small range of $\mathcal{E}$ values before these global bifurcation we observe bistability: trajectories starting close to the saddle-point of the first external cavity modes are attracted by a delay induced limit cycle, whereas trajectories starting elsewhere (attractor's plane) end up in a stable node. In the output of the laser this delay induced limit cycle is manifested by regular pulse packages as they are depicted in Figure **5e**. Looking at the phase space projections of Figure **6e** it can be seen that starting from a maximum intensity point of one pulse package the excursion

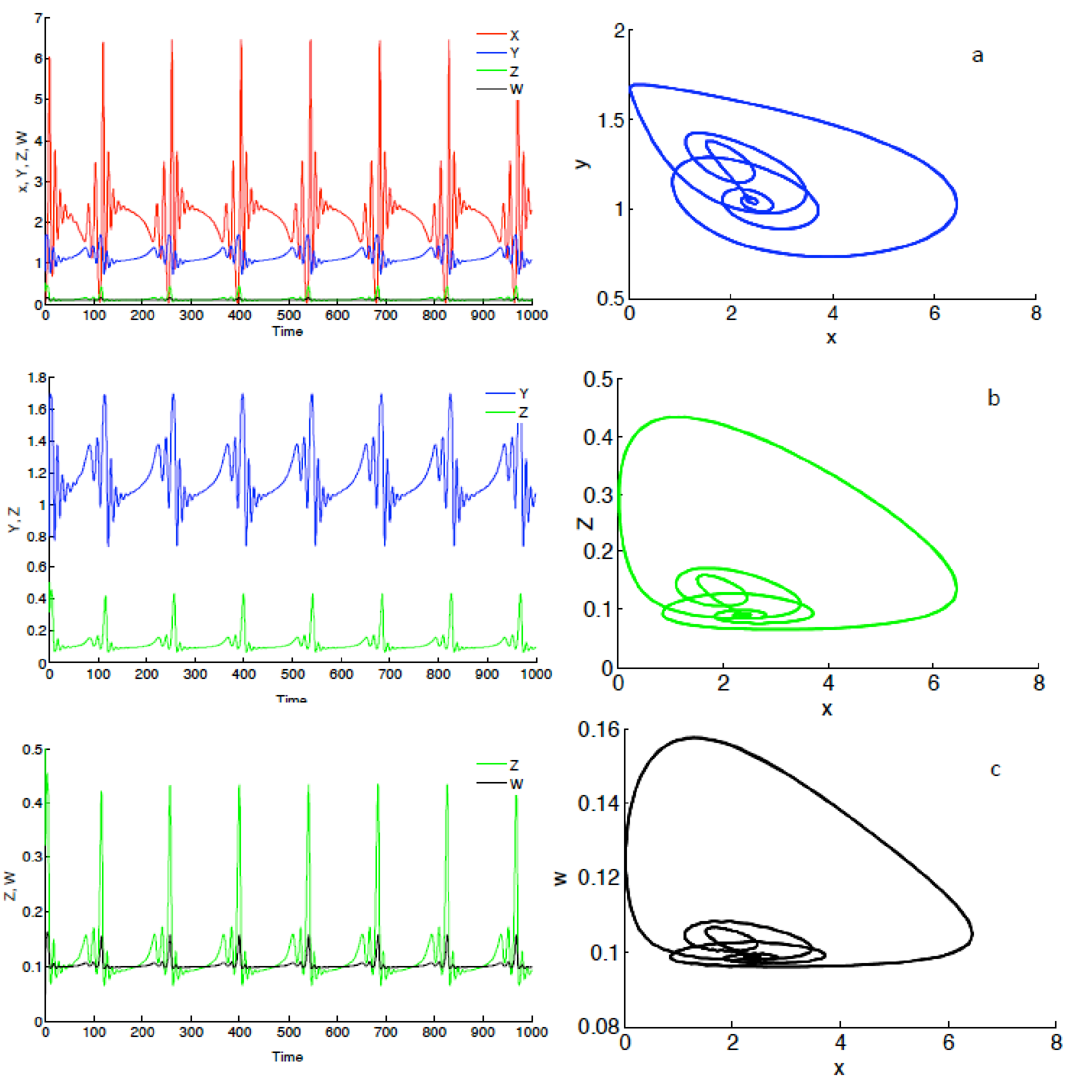

Figure 6: Time series (column 1), phase space attractors of the trajectory onto planes spanned by the photon density *x* and the occupation probability ground and excited states (*y* and *z*), and carrier density *w* in WL (column 2). Rows (a–c) correspond to Ɛ = 0.348, δo = 0.18 as indicated by column 1 lines (a–c) in the time series for small α = 0.9 and Θ = 0.

through the (x, y, w)-3D-space is similar to the turn-on dynamics of the QD-laser as the trajectory spirals towards a certain point in phase space.

The description of the dynamics in QD lasers requires the inclusion of the interaction between discrete states localized at the QDs and the continuous ground and excite states at higher energies within the WL. Since we are interested in the investigation of the laser regime, i.e., the WL carrier density is very high, the capture dynamics within the QD-WL structure is dominated. The slow and fast capture for electron from WL into QD states (ground and excite) are calculated as a function of the injection current into WL. Figure **1a** and1b, shows the scheme of the QD-WL structure illustrating the considered the capture of an electron from a WL with the QD into an energetically higher state and between ground and excite states.

Outside the locking region, the slowly varying field amplitude E of the QD laser oscillates with a frequency close to the input detuning w_o resulting in a periodic modulation of S with one maximum and four minimum (gray regions in Figure **6a**). Approaching the periodic behavior from the outside of the locking region for small Ɛ, the flow on the large limit cycle slows above the small cycles fast, where the spikes will appear and then makes a quick excursion along the other part of the periodic orbit. Figure **6b** depicts the dynamics close to the bifurcation (see Figure **3**). The time series now displays regular pulsing of S, and the attractors on to the phase plane shows the big limit-cycle. This can be seen from Figures **6a-c** by noting that the output is labeled by X, Y, Z and W.

4.2. Impact of the Phase-Amplitude Coupling (Increase α-Factor)

To far the discussion was limited to the regime of feedback strengths Ɛ where only one external cavity mode, i.e., the one that can be continued out of the solitary laser solution, is available to the QD laser. This is proven by Figure **4** that depicts the solutions for the Eqs. 3(a-e). Now, the impact of the phase-amplitude coupling on the dynamics of the optical feedback QD laser is analyzed. In the introduction of this paper, it was discussed that in models, in which the phase-amplitude coupling is described by a constant α-factor, the dynamics of QD lasers is best approximated by small values of α, while QW lasers typically have large α-factors [44]. In Figure **7a, b**, show at two values of Θ the same dynamics of the output laser. Thus, For QD

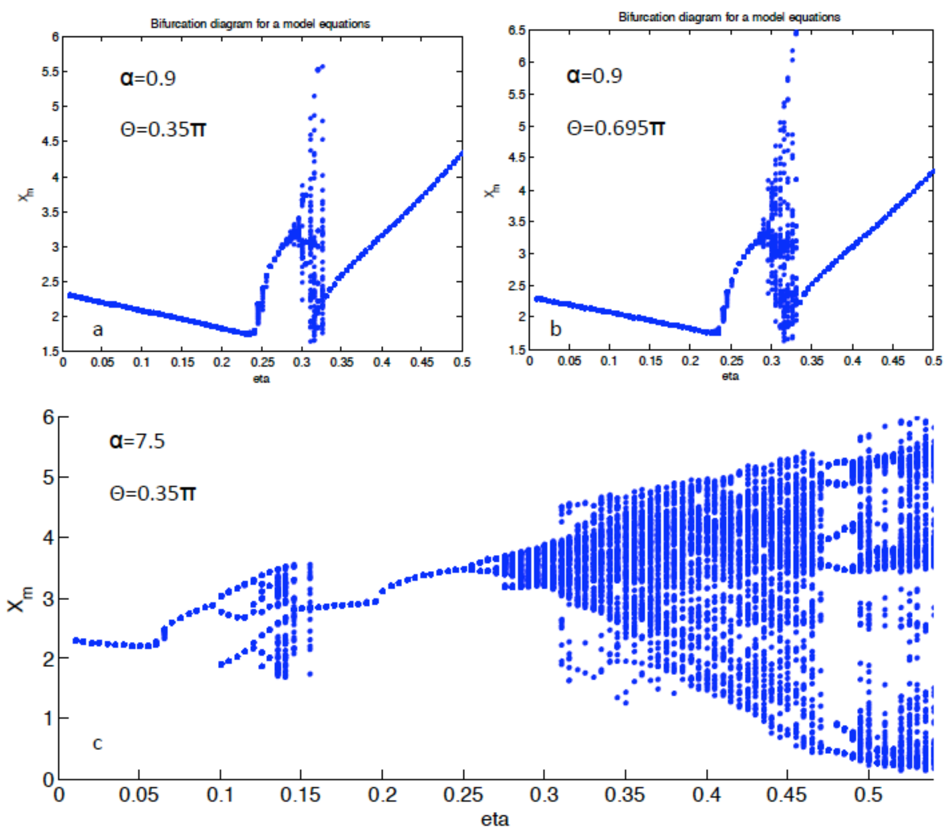

Figure 7: Bifurcation diagrams of the photon density x of the possible external cavity modes in dependence of the feedback strength Ɛ for small α = 0.9 (a and b are compared between two values of Θ) and large α = 7.5 (c).

lasers, the locking tongue remains nearly symmetrical with respect to α. (Figure **6a**) is compared to its dynamics with large α = 7.5 (Figure **7c**). The dynamics for a small α-factor was already discussed in the previous section. (Figure **7a** is identical to Figure **4**) With increasing α, the phase-locking range shrinks, because the upper supercritical Hopf bifurcation line bends towards zero. Thus, pulsating behavior of the photon is found for Ɛ = 0.06 at Θ = 0.35π. This was observed experimentally in QW lasers [45]. This permits to conclude that QD lasers have indeed a smaller phase-amplitude coupling than QW lasers, which is supported by more complex modeling approaches [46, 47]. For QD models, in which the phase-amplitude coupling is simply described by a constant α-factor, this may be modeled by using small values for α, i.e. α ≤ 2. Such a choice of α avoids that the upper supercritical Hopf bifurcation line crosses the zero detuning line.

Further, at $\alpha = 7.5$ and when $\mathcal{E} = 0.48$ a new pair of external cavity modes is born in a saddle-node bifurcation. In Figure **7c** show the linewidth enhancement factor α clearly display desynchronized dynamics. Thus, a new stable fixed point (node) as well as a saddle-point are available to the system dynamics. As a consequence we observe another drastic change of the laser dynamics towards stable cw operation: at the bifurcation point $\mathcal{E} = 0.16$ a global bifurcation takes place. Due to the typical scaling, we presume it to be a homoclinic bifurcation of a limit cycle. This can be seen in the bifurcation diagram in Figure **6c** that show only one single branch beyond $\mathcal{E} = 0.16$. In a small range of $\mathcal{E}$ values before these global bifurcation we observe bistability: trajectories starting close to the saddle-point of the first external cavity mode are attracted by a delay induced limit cycle, whereas trajectories starting elsewhere end up in a stable node.

CONCLUSION

In this paper we have controlled that the nonlinear properties of a QD laser are influenced not only by the linewidth enhancement factor α but also by the phase Θ as function of the bias current δo, delayed time τ and feedback strength Ɛ. In our QD laser dimensionless model we obtain different dynamics that change with the bias current δ_o, delayed time τ and feedback strength Ɛ and the considered QD-QW structure. Therefore, we can investigate changes of these parameters without changing the system parameters. Within this model we have identified both analytically and numerically the most important parameters that determine the sensitivity of the QD laser to optical feedback. We propose that the stability of the laser towards optical feedback can be significantly increased by a small α-factor, a high bias current at periodic values of phase Θ = [0, 0.35π, 0.695π,…]. Such a choice of the parameters leads to a higher damping of the relaxation oscillations. Thus, we can conclude that the strongly damped relaxation oscillations of the QD laser cause its lower sensitivity to optical feedback.

REFERENCES

[1] Fischer I, Liu Y and Davis P. Synchronization of chaotic semiconductor laser dynamics on subnanosecond time scales and its potential for chaos communication. Phys Rev A 62; 011801 (2000). http://dx.doi.org/10.1103/PhysRevA.62.011801

[2] Heil T, Mulet J, Fischer I, Mirasso CR, Peil M, Colet P and Elsäßer W. On/off phase shift keying for chaos-encrypted communication using external-cavity semiconductor lasers, IEEE J. Quantum Electron 2002; 38: 1162-1170. http://dx.doi.org/10.1109/JQE.2002.801950

[3] Vicente R, Mirasso CR and Fischer I. Simultaneous bidirectional message transmisson in a chaos-based communication scheme. Opt Lett 2007; 32: 403-405. http://dx.doi.org/10.1364/OL.32.000403

[4] Argyris A, Syvridis D, Larger L, Annovazzi-Lodi V, Colet P, Fischer I, *et al*. Chaos-based communications at high bit rates using commercial fibre-optic links, Nature 2005; 438: 343-346. http://dx.doi.org/10.1038/nature04275

[5] Viktorov EA, Mandel P and Huyet G. Long-cavity quantum dot laser. Opt Lett 2007; 32: 1268-1270. http://dx.doi.org/10.1364/OL.32.001268

[6] Kinzel W, Englert A and Kanter I. On chaos synchronization and secure communication. Phil Trans R Soc 2010; A 368: 379-389.

[7] Radziunas M, Glitzky A, Bandelow U, Wolfrum M, Troppenz U, Kreissl J, *et al.* Improving the Modulation Bandwidth in Semiconductor Lasers by Passive Feedback. IEEE J Sel Top Quantum Electron 2007; 13: 136-142. http://dx.doi.org/10.1109/JSTQE.2006.885332

[8] Tronciu VZ. Excitability and coherence resonance of a DFB laser with passive dispersive reflector. Moldavian Journal of the Physical Sciences 2008; 7: 516.

[9] Schikora S, Hövel P, Wünsche HJ, Schöll E, and Henneberger F. Alloptical noninvasive control of unstable steady states in a semiconductor laser. Phys Rev Lett 2006; 97: 213902. http://dx.doi.org/10.1103/PhysRevLett.97.213902

[10] Flunkert V and Schöll E. Suppressing noise-induced intensity pulsations in semiconductor lasers by means of time-delayed feedback. Phys Rev 2007; E 76, 066202.

[11] Dahms T, Hövel P and Schöll E. Control of unstable steady states by extended time-delayed feedback. Phys Rev 2007; E 76: 056201.

[12] Dahms T, Hövel P and Schöll E. Stabilizing continuous-wave output in semiconductor lasers by time-delayed feedback. Phys Rev 2008; E 78: 056213.

[13] Fiedler B, Yanchuk S, Flunkert V, Hövel P, Wünsche HJ and Schöll E. Delay stabilization of rotating waves near fold bifurcation and application to all-optical control of a semiconductor laser. Phys Rev 2008; E 77: 066207.

[14] Dahms T, Flunkert V, Henneberger F, Hövel P, Schikora S, Schöll E and Wünsche HJ. Noninvasive optical control of complex semiconductor laser dynamics. Eur Phys J ST 2010; 191: 71. http://dx.doi.org/10.1140/epjst/e2010-01342-8

[15] Schöll E and Schuster HG (Editors): Handbook of Chaos Control (WileyVCH, Weinheim, 2008), Second completely revised and enlarged edition.

[16] Schöll E, Hövel P, Flunkert V and Dahlem MA. Time-delayed feedback control: from simple models to lasers and neural systems, in Complex timedelay systems: theory and applications, edited by Atay FM. (Springer, Berlin, 2010); pp. 85-150.

[17] Hicke K, D'Huys O, Flunkert V, Schöll E, Danckaert J and Fischer I: Mismatch and synchronization: Influence of asymmetries in systems of two delay-coupled lasers. Phys Rev 2011; E 83: 056211.

[18] Dahms T. Synchronization in Delay-Coupled Laser Networks, Ph.D. thesis, Technische Universität Berlin 2011.

[19] Dahms T, Lehnert J and Schöll E. Cluster and group synchronization in delay-coupled networks. Phys Rev 2012; E 86: 016202.

[20] Flunkert V, D'Huys O, Danckaert J, Fischer I and Schöll E. Bubbling in delay-coupled lasers. Phys Rev 2009; E 79: 065201 (R).

[21] Flunkert V. Delayed complex systems and applications to lasers, Ph.D. thesis, TU-Berlin 2010.

[22] Soriano MC, García-Ojalvo J, Mirasso CR and Fischer I. Complex photonics: Dynamics and applications of delay-coupled semiconductors lasers. Rev Mod Phys 2013; 85: 421-470. http://dx.doi.org/10.1103/RevModPhys.85.421

[23] Su H, Zhang L, Gray AL, Wang R, Newell TC, Malloy KJ and Lester LF. High external feedback resistance of laterally loss-coupled distributed feedback quantum dot semiconductor lasers. IEEE Photonics Technol. Lett 2003; 15: 1504-1506. http://dx.doi.org/10.1109/LPT.2003.818627

[24] Huyet G, O'Brien D, Hegarty SP, McInerney JG, Uskov AV, Bimberg D, *et al.* Quantum dot semiconductor lasers with optical feedback. Phys Stat Sol 2004; (b)201: 345-352.

[25] O'Brien D, Hegarty SP, Huyet G, McInerney JG, Kettler T, Lämmlin M, *et al.* Feedback sensitivity of 1.3 μm InAs/GaAs quantum dot lasers, Electronics Letters 2003; 39: 1819-1820. http://dx.doi.org/10.1049/el:20031153

[26] Carroll O, O'Driscoll I, Hegarty SP, Huyet G, Houlihan J, Viktorov EA, *et al.* Feedback induced instabilities in a quantum dot semiconductor laser. Opt Express 2006; 14: 10831-10837. http://dx.doi.org/10.1364/OE.14.010831

[27] Carroll O, Hegarty SP, Huyet G and Corbett B. Length dependence of feedback sensitivity of InAs/GaAs quantum dot lasers. Electron Lett 2005; 41: 39-40. http://dx.doi.org/10.1049/el:20051838

[28] Carroll O, O'Driscoll I, Hegarty SP, Huyet G, Houlihan J, Viktorov EA and Mandel P. Feedback induced instabilities in a quantum dot semiconductor laser. Opt Express 2006; 14: 10831-10837. http://dx.doi.org/10.1364/OE.14.010831

[29] Huyet G, O'Brien D, Hegarty SP, McInerney JG, Uskov AV, Bimberg D, *et al.* Quantum dot semiconductor lasers with optical feedback. Phys Stat Sol 2004; (b)201: 345-352.

[30] Otto C, Lüdge K and Schöll E. Modeling quantum dot lasers with optical feedback: sensitivity of bifurcation scenarios. Phys Stat sol 2010; (b)247: 829-845.

[31] Otto C, Lüdge K, Vladimirov AG, Wolfrum M and Schöll E. Delay induced dynamics and jitter reduction of passively mode-locked semiconductor laser subject to optical feedback. New J Phys 2012; 14: 113033. http://dx.doi.org/10.1088/1367-2630/14/11/113033

[32] Globisch B, Otto C, Schöll E and Lüdge K. Influence of carrier lifetimes on the dynamical behavior of quantum-dot lasers subject to optical feedback. Phys Rev E 2012; 86: 046201. http://dx.doi.org/10.1103/PhysRevE.86.046201

[33] Voignier V. 'stabilization of self-focusing instability in wide-aperture semiconductor laser. Phys Rev A 2002; 65(5): Article Number: 053807(5 pages).

[34] Uskov A, Boucher Y, Bihan JL and McInerney J. Appl Phys Lett 1998; 11: 1499. http://dx.doi.org/10.1063/1.122185

[35] Sugawara M, Mukai K and Shoji H. Appl Phys Lett 1997; 71: 2791. http://dx.doi.org/10.1063/1.120135

[36] Otto C, Globisch B, Ludge K, Scholl E and Erneux T. Int J Bif Chaos, accepted 2012.

[37] Haegeman B, Engelborghs K, Roose D, Pieroux D and Erneux T. Phys Rev 2002; E66: 046216.

[38] Heil T, Fischer I, Elsaer W, Krauskopf B, Green K and Gavrielides A. Phys Rev 2003; E67: 066214.

[39] Green K. Phys Rev 2009; E79: 036210.

[40] Uskov AV, Boucher Y, Bihan JL and McInerney J. Theory of a self-assembled quantum-dot semiconductor laser with auger carrier capture: Quantum efficiency and nonlinear gain. Appl Phys Lett 1998; 73(11): 1499-1501. http://dx.doi.org/10.1063/1.122185

[41] Ludge K, Aust R, Fiol G, Stubenrauch M, Arsenijevic D, Bimberg D, *et al.* IEEE J Quantum Electron 2010; 46: 1755. http://dx.doi.org/10.1109/JQE.2010.2066959

[42] Otto C, Ludge K and Scholl E. Phys Stat Sol 2010; (b)247: 829.

[43] Otto C, Globisch B, Ludge K, Scholl E and Erneux T. Int J Bif Chaos, accepted 2012.

[44] Kane DM and Shore KA. (Editors): Unlocking Dynamical Diversity: Optical Feedback Effects on Semiconductor Lasers (Wiley VCH, Weinheim, 2005). http://dx.doi.org/10.1002/0470856211

[45] Wieczorek S, Simpson TB, Krauskopf B and Lenstra D. Global quantitative predictions of complex laser dynamics. Phys Rev 2002; E65: 045207. http://dx.doi.org/10.1103/physreve.65.045207

[46] Lingnau B, Lüdge K, Chow WW and Schöll E. Failure of the α-factor in describing dynamical instabilities and chaos in quantum-dot lasers. Phys Rev 2012; E86: 065201(R).

[47] Lingnau B, Chow WW, Schöll E and Lüdge K. Nonequilibrium dynamics of quantum-dot lasers under optical injection and feedback. New J Phys In preparation 2013.

Received on 31-10-2015 Accepted on 07-12-2015 Published on 31-07-2016

DOI: http://dx.doi.org/10.12974/2311-8792.2016.04.2